Analyst

Accepted Manuscript

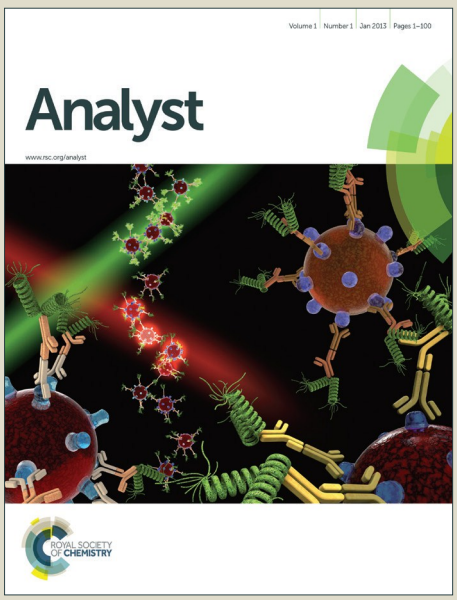

ROYAL SOCIETY OF CHEMISTRY

www.rsc.org/analyst

Analyst

Dynamic Article Links ►

Cite this: DOI: 10.1039/c0xx00000x

www.rsc.org/xxxxxx

COMMUNICATION

Capillarity-driven Blood Plasma Separation on Paper-based Devices

Shantimoy Kar[1], Tapas K. Maiti[1,2] and Suman Chakraborty[1,3]

Received (in XXX, XXX) Xth XXXXXXXXX 20XX, Accepted Xth XXXXXXXXX 20XX
DOI: 10.1039/b000000x

We demonstrate capillarity-driven plasma separation from whole blood on simple paper-based H-channels. This methodology, unlike other reported techniques, does not necessitate elaborate and complex instrumentation, and the needs for expensive consumables. We believe that this technique will be ideally suited to be implemented in rapid and portable blood diagnostic devices designed to be operative at locations with limited resources.

Separation of blood plasma has paramount importance in diagnosing several bio-analytes suspended in blood. To achieve an efficient plasma separation, conventional methods like centrifugation or magnetic separation[1] are followed in standard laboratory based techniques. Recently, paper-based flow strips have emerged as highly effective platforms for point-of-care (POC) diagnostics[2–4]. Such paper-based devices have ample advantages like ease and economy of fabrication, as well as functionalities at locations having limited resources.

Numerous techniques have been reported in the literature for the detection of bio-analytes on paper based devices. Amongst them, the colorimetric approach is more common as the readings may be visible through naked eye. The fluorescence-based[5,6] , nanoparticles-based[7], and electrochemical sensing[8,9] techniques have been well-explored on paper-based devices with higher sensitivity. However, these techniques have not turned out to be widely acceptable due to involved complex instrumentations (e.g., optics, fluorescence detector, specific light source, integrated battery etc.), which enhances the operating expenses. One major challenge behind the implementation of the colorimetric detection technique lies in differentiating the colorimetric signals from the intense red color of blood. Currently available commercial devices use RBC specific membranes (to which RBCs specifically adhere)[10] , which only allow plasma to pass through into the paper-strip. Usage of such RBC-specific membranes, thus, assists to detect the analytes present in plasma solutions by filtration of RBC (through RBC specific membrane). As a consequence, application of such RBC-specific membranes is essential for the detection of any sort of analytes from plasma, which increases the cost of the device significantly. In this context, it is important to engineer a low-cost yet effective platform which will have an integrated setup for separating RBCs and plasma from the whole blood and will accordingly detect the analytes of interest. There have been attempts made by several research groups to separate RBCs on paper-based devices by using the agglutination reagent[11] and electrochemical methods[12]. Though the aforementioned techniques are reported to show efficient separation of blood plasma from whole blood, these technologies suffer from certain limitations in a sense that they necessitate the usages of expensive chemicals/ consumables as well as sophisticated instrumentation.

Here, we demonstrate a new inexpensive methodology for the separation of plasma from whole blood. Our methodology involves the capillarity driven diffusion of blood samples. The 2-dimensional paper based network (2DPN)[13] has been widely explored in literature for several applications like controlled transport of chemicals[14] and subsequent signal amplification during detection using the gold nanoparticles[15]. The 2DPN device does not demand any external pump or pressure control system to actuate the fluid flow. To separate the plasma from whole blood, we have used an H-filter[13] and have concomitantly exploited the capillarity-driven transport of blood on paper-based devices. There are reports which illustrate the usage of 2DPN devices to implement lateral flow strip assay[16]. In this particular work, we present an inexpensive method for blood separation (specifically red color separation) which shows favourable separation efficiency and reproducible results.

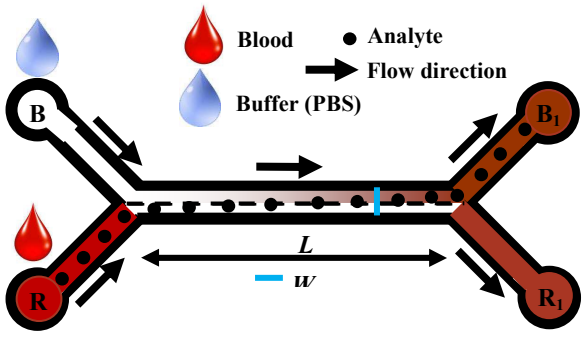

Figure 1: Schematic representation of the device set-up, where the blood and dilution buffer are dispensed in reservoirs R and B, respectively. At the end of the experiments, it is seen that the plasma solution is getting separated in reservoir B_1, whereas the reservoir R_1 contains the separated RBCs. The black arrow shows the direction of fluid flow in the device. Device dimensions are: W=5 mm, H = 180 μm (channel height), L= 3 cm. Diameters of the all the reservoirs (R, B, R_1, B_1) are 6 mm. Width of the conduit connecting each reservoir with the main channel is 2 mm.

The schematic of the H-channel is shown in figure 1. After printing the particular design on standard laboratory grade filter paper (Whatmann grade 4), we cut the H-filter device through a knife following an origami-based protocol[17,18]. All the experiments were carried out using human blood sample following pertinent ethical guidelines. Hematocrit is known to significantly affect the rheological properties of blood[19,20], but the separation efficiency (η) of our device is almost invariant with the variation of hematocrit value of blood (as shown in Figure S1 of Electronic Supplementary Information (ESI)). We have executed all the experiments for a representative hematocrit value of $(37 \pm 1)\%$ (hematocrit value of healthy persons usually vary in a range of 35-45%).

During the experimentation, images have been captured (as shown in figure 2a) with a digital camera (Nikon Coolpix L810). Thereafter, the captured images have been processed using the ImageJ software. During analysis, we have measured the grayscale intensity per unit area at specific location of a particular image. The grayscale intensity has been averaged out over a rectangular region of (7 pixels×60 pixels). During the experimentation, 50 μl of blood sample and 50 μl of PBS buffer solution (pH~7.4, 1X) are respectively kept at R and B reservoirs. We have analyzed the images at a particular location just after the blood has reached the same, so that the effect of evaporation can be neglected.

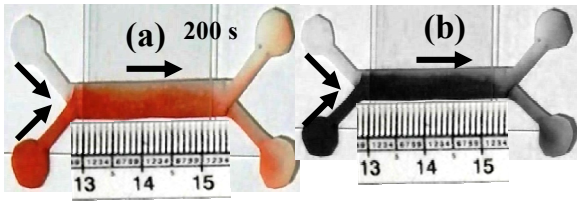

Figure 2: **(a)** Real time image of the device after the end of the experiments (i.e. at 200 seconds), when blood has reached to the end reservoirs; (b) the same image after processing through ImageJ software, from which it is evident that how the width of the red zone gets reduced along the length of the channel.

Paper-matrix is composed of enormous number of cellulose fibres which are randomly distributed. The flow through such type of paper-matrix occurs due to the capillary imbibitions through the inter-fibre passages. During the experimentations, both the fluids (blood and PBS) imbibe through the random network of cellulose fibres. In due course of flow, blood and PBS flow simultaneously in the straight part of the channel. During the flow, lighter molecules (having low molecular weight) suspended within the blood stream diffuse into the PBS stream. One may intuitively expect that at the end of the linear part of the device, the lighter molecules are supposed to enrich in the buffer stream. As the fluid traverses through the channel, the lighter molecules are expected to be diffused more and finally collected at reservoir B_1. The reservoir R_1 contains more red stain as compared to that of reservoir B_1. From figure 2a, it is evident that the intensity of red color is more at the reservoir R_1, in comparison to that of the reservoir B_1. Figure 2b provides more clarity regarding the red color separation. In this entire investigation, the separation of plasma is solely guided by the capillarity-driven diffusion of analyte molecules. It is known that the diffusion coefficient of glucose molecule is higher (by an $O \sim 10^2$) as compared to that of a RBC; thereby triggering diffusion based intrinsic separation.

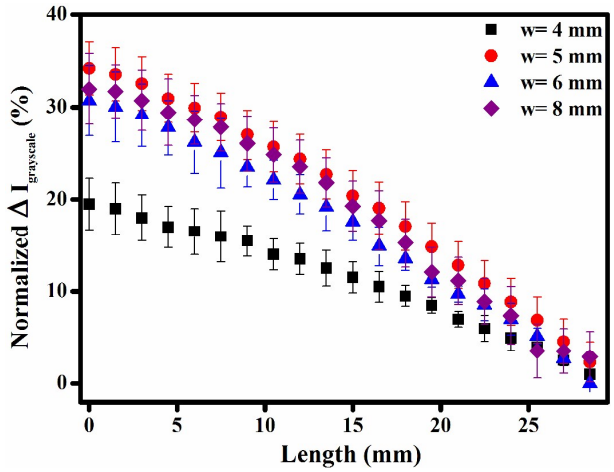

Figure 3: Variation of the grayscale intensity of the red zone along the length of the channel, for different widths of the paper-based devices. Higher value of grayscale intensity signifies more faint coloration at a particular point. The above study has been executed for a channel length of 3 cm. The error bar represents the standard deviation (s.d.) obtained from five repeated sets of experimental data.

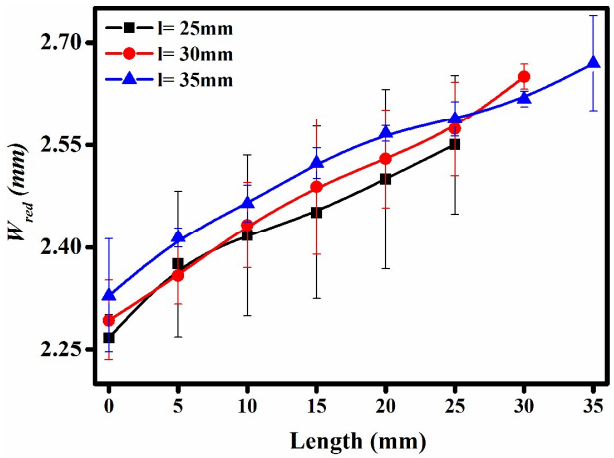

Figure 4: Variation of the width of the red zone (in terms of grayscale intensity) along the length of the channel. Entire analysis has been done at the instant when the fluid front has just reached a specific location. From the above plot, it is seen that the variation of length does not affect the extent of red zone for a particular length of the channel. The experiments have been carried out for a specific channel width of 5 mm. The error bars

represent the standard deviations (s.d.) of the results from five repeated sets of experiments.

We have investigated the effect of width and length variation of the H-filter based paper devices, in an effort to optimize the separation efficiency of the device. In figure 3, we have quantified the variation of grayscale intensity ($\Delta I_{grayscale}$) along the length of the H-filter devices. It is seen that the change of grayscale intensity gradually reduces as we proceed towards the downstream part of the channel, indicating diffusion of the blood stream through the PBS stream. From figure 3, it is evident that the change in grayscale intensity values shows maxima for a channel width of 5 mm (34.2%) as compared to the other dimensions i.e. for W = 4 mm, maximum $\Delta I_{grayscale}$ =19.5%; for W = 6 mm, maximum $\Delta I_{grayscale}$ =30.6%; and for W = 8 mm, maximum $\Delta I_{grayscale}$ =31.9%). Considering the error bars it is evident that the values of $\Delta I_{grayscale}$ do not show any perceptible changes for the device having larger width than 5 mm. This may be attributed to the fact that since the characteristic length scale (here it is the height) of the channel is of the order of microns, the lateral dimension becomes inconsequential beyond a threshold limit. For that reason, we have chosen 5 mm width of the device for rest of the experiments. We have illustrated the effect of length variation in figure 4. It is seen that the width of red zone (W_{red}) gradually increases along the straight path of the channel and there is no significant variation as we vary the length of the channel. Considering the commercial potential of such devices, we choose a length of the device i.e. 3 cm, which is good enough in terms portability.

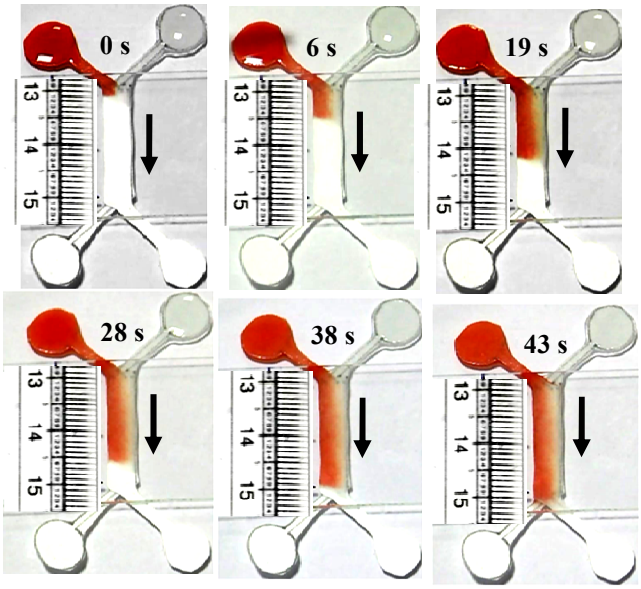

Figure 5: Real time image sequences showing how the blood stream diffuses into the buffer stream and accordingly the blood strain covers the entire width of the paper channel.

We have defined a separation efficiency parameter as: $\eta = (I_R - I_{B1})/I_R$, where I_R and I_{B1} are the intensities (grayscale values) of the R and B_1 reservoirs respectively, i.e. separation efficiency signifies the change in grayscale intensities with respect to the same of 'R' reservoir. Physically, it denotes the fraction of colour reached in 'B_1' reservoir with respect to that of 'R' reservoir. We have found that the separation efficiency is 75.4 ± 9.1% for a device having a width of 5 mm and length 3 cm. From figure 5, it is clearly seen that the blood stream diffuses into the buffer stream and accordingly plasma is separated from the blood. However, according to our definition of η, it solely depends on the grayscale intensity values of the reservoirs. Hence, it is difficult to assess the extent of plasma being separated out in the process. To make an assessment about the total amount of enriched plasma at the reservoir B_1, we have performed separate independent experiments in which we have detected the glucose content from the separated plasma collected at the same reservoir (for details see ESI). Since there are many analytes and proteins present in the plasma, the detection of a particular analyte (here for our case it is glucose) is only an indicative estimation of separated plasma. We have measured the glucose at the reservoir B_1 by employing a reagent (glucose oxidase + peroxidase + 4-Amino Anti-Pyrene), merely for the purpose of standardization of the adopted technique. According to the calibration curve (Figure S2 of ESI), the value of separation efficiency (η) is found to be $(71.45 \pm 4.04)\%$ (shown in Table 1 of ESI). So, it is worth to mention here that the values of separation efficiency obtained from both intensity-based technique and calibration curve are comparable. The glucose level of the collected plasma (calculated from the separation efficiency = 75.4%) differs from the actual glucose level by a value within 10% (as shown in Table 1 of ESI), which compares favourably with the errors incurred in other reported techniques [10–12], albeit the fact that the other techniques use more expensive platforms for the same purpose. Results with such accuracy may be well acceptable within the purview of low-cost POC devices.

In summary, we have fabricated a frugal paper-based platform which efficiently separates blood plasma from whole blood sample. The simple origami-based fabrication of paper devices and the elegant methodology of separation (requires very minimal resources) collectively make the device suitable for operation in locations with limited resources. This method requires none of the state of the art instrumentations, nor any trained personnel, nor any kind special sophisticated laboratory environment, and may potentially act as a fundamental premise for detection of diseased conditions in blood samples in a rapid, efficient, and low cost paradigm.

Notes and references

[1]Advanced Technology Development Centre, Indian Institute of Technology Kharagpur, Kharagpur-721302; [2]Department of Biotechnology, Indian Institute of Technology Kharagpur, Kharagpur-721302; [3]Department of Mechanical Engineering, Indian Institute of Technology Kharagpur, Kharagpur-721302, India.
Email: suman@mech.iitkgp.ernet.in

Acknowledgement: S.K would like to thank Council of Scientific and Industrial Research (CSIR), India for his research

fellowship. SK acknowledges the assistance of Mr. Jai Prakash Gautam from Indian Institute of Technology Patna at the initial stage of the work.

References:

1. J. Svoboda, *J. Magn. Magn. Mater.*, 2000, **220**, 103–105.
2. A. K. Yetisen, M. S. Akram, and C. R. Lowe, *Lab Chip*, 2013, **13**, 2210–51.
3. V. Gubala, L. F. Harris, A. J. Ricco, M. X. Tan, and D. E. Williams, *Anal. Chem.*, 2012, **84**, 487–515.
4. X. Li, D. R. Ballerini, and W. Shen, *Biomicrofluidics*, 2012, **6**, 11301–1130113.
5. N. K. Thom, G. G. Lewis, K. Yeung, and S. T. Phillips, *RSC Adv.*, 2014, **4**, 1334–1340.
6. M. He and Z. Liu, *Anal. Chem.*, 2013, **85**, 11691–11694.
7. W. Zhao, M. M. Ali, S. D. Aguirre, M. A. Brook, and Y. Li, 2008, 8431–8437.
8. P. Rattanarat, W. Dungchai, W. Siangproh, O. Chailapakul, and C. S. Henry, *Anal. Chim. Acta*, 2012, **744**, 1–7.
9. W. Dungchai, O. Chailapakul, and C. S. Henry, *Anal. Chem.*, 2009, **81**, 5821–5826.
10. T. Songjaroen, W. Dungchai, O. Chailapakul, C. S. Henry, and W. Laiwattanapaisal, *Lab Chip*, 2012, **12**, 3392.
11. X. Yang, O. Forouzan, T. P. Brown, and S. S. Shevkoplyas, *Lab Chip*, 2012, **12**, 274.
12. J. Noiphung, T. Songjaroen, W. Dungchai, C. S. Henry, O. Chailapakul, and W. Laiwattanapaisal, *Anal. Chim. Acta*, 2013, **788**, 39–45.
13. J. L. Osborn, B. Lutz, E. Fu, P. Kauffman, D. Y. Stevens, and P. Yager, *Lab Chip*, 2010, **10**, 2659–2665.
14. E. Fu, S. A. Ramsey, P. Kauffman, B. Lutz, and P. Yager, *Microfluid. Nanofluidics*, 2011, **10**, 29–35.
15. E. Fu, P. Kauffman, B. Lutz, and P. Yager, *Sens. Actuators. B. Chem.*, 2010, **149**, 325–328.
16. E. Fu, T. Liang, J. Houghtaling, S. Ramachandran, S. A. Ramsey, and B. Lutz, *Anal. Chem.*, 2011, **83**, 7941–7946.
17. S. Chen, Y. Liao, and J. Yang, in *Internal Conference on Miniaturized Systems of Chemictry and Life Sciences*, 2013, pp. 1583–1585.
18. H. Liu and R. M. Crooks, *J. Am. Chem. Soc.*, 2011, **133**, 17564–17566.
19. S. Kar, M. Dash, T. K. Maiti, and S. Chakraborty, *Analyst*, 2015, **140**, 1432–1437.
20. J. J. Bishop, A. S. Popel, M. Intaglietta, and P. C. Johnson, *Biorheology*, 2001, **38**, 263–274.

